Disorder and funneling effects on exciton migration in treelike dendrimers

Subhadip Raychaudhuri,[1] Yonathan Shapir,[1] and Shaul Mukamel[2]
[1]*Department of Physics and Astronomy, University of Rochester, Rochester, New York 14627*
[2]*Department of Chemistry, University of Rochester, Rochester, New York 14627*
(Received 27 June 2001; published 16 January 2002)

The center-bound excitonic diffusion on dendrimers subjected to several types of nonhomogeneous funneling potentials is considered. We first study the mean first passage time (MFPT) for diffusion in a linear potential with different types of correlated and uncorrelated random perturbations. Increasing the funneling force, there is a transition from a phase in which the MFPT grows exponentially with the number of generations g to one in which it does so linearly. Overall the disorder slows down the diffusion, but the effect is much more pronounced in the exponential compared to the linear phase. When the disorder gives rise to uncorrelated random forces there is, in addition, a transition as the temperature T is lowered. This is a transition from a high-T regime in which all paths contribute to the MFPT to a low-T regime in which only a few of them do. We further explore the funneling within a realistic nonlinear potential for extended dendrimers in which the dependence of the lowest excitonic energy level on the segment length was derived using the time-dependent Hatree-Fock approximation. Under this potential the MFPT grows initially linearly with g but crosses over, beyond a molecular-specific and T-dependent optimal size, to an exponential increase. Finally we consider geometrical disorder in the form of a small concentration of long connections as in the *small world* model. Beyond a critical concentration of connections the MFPT decreases significantly and it changes to a power law or to a logarithmic scaling with g, depending on the strength of the funneling force.

DOI: 10.1103/PhysRevE.65.021803 PACS number(s): 36.90.+f, 05.40.Fb, 31.70.Hq

I. INTRODUCTION

Extended dendrimers (Fig. 1) are nanoscale Cayley-treelike supermolecules that exhibit an energy gradient from the periphery to the center of the molecule. Their unique hierarchical self-similar structure can be described by three ingredients: the basic building block (e.g., phenyl acetylene linear segment), the branching of the end points, and the number of generations. The number of basic elements grows exponentially with the number of generations g, and the number of elements at the periphery of the molecule is comparable to the number of bulk elements.

Recent theoretical and experimental studies [1–4] have shown that the electronic excitations of these dendrimers are spatially localized within each segment. For these dendrimers, lengthening of the linear tree branches towards the core leads to a hierarchy of localization lengths. Hence the exciton energy decreases with generation from the periphery to the core. This *energy funnel* combined with the large number of absorbing elements at the periphery makes these dendrimers potentially efficient single molecule antenna systems [5]. Excitons created upon optical excitation of the shortest linear segments at the periphery diffuse through the intermediate regions, finally reaching the core where an energy trap is located. Excitation transfer proceeds via Coulomb interaction and may be described by the Frenkel exciton model. Theoretical studies [6] have focused on calculating the time it takes for an exciton generated at the surface to reach the core. This trapping time is a direct measure of the efficiency of the antenna. Its dependence on the number of generations g and the funneling driving force was calculated.

These studies, which were able to capture some important features of excitonic diffusion on dendrimers, assumed that all the tree branches (namely, the linear polymeric chains) of a given generation are identical. This implies that the exciton energies are fixed. In reality interaction with the solvent and intramolecular vibrations induce slow (quenched) fluctuations in the energy. (Nonlinear [7] and single molecule [8] spectroscopy typically show nanosecond to millisecond bath motions whereas the exciton trapping times are typically in the picosecond range [5,9]).

On a more fundamental level, diffusion in disordered media is an active field of statistical physics [10]. Different forms of correlations among energy levels were considered and nontrivial behaviors, such as the difference between the typical and the average diffusion, anomalous scaling, and others, were found in some cases. Independently, theoretical investigations of dynamics on Cayley trees (or Bethe lattices) lead to many interesting results. Exact solutions exist for some problems and bear important consequences. Directed polymer on Cayley trees is one of the interesting examples where a spin-glass-like transition was predicted [11]. As shown below, the problem of diffusion on a disordered Cayley tree exhibits such a transition as well and thus has a

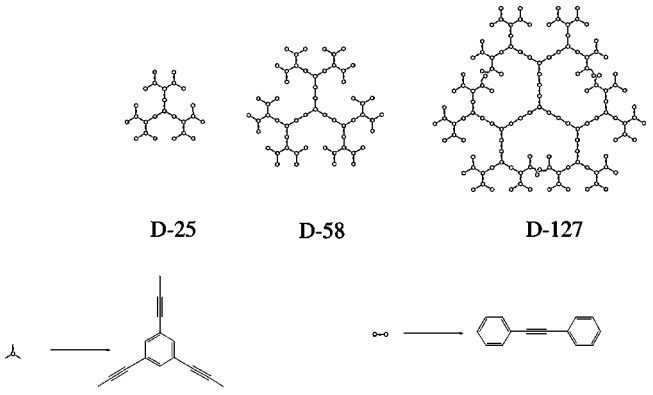

FIG. 1. Extended phenylacetylene dendrimers with increasing total number of generations.

TABLE I. The different dendrimer models considered in this work and the relations between them.

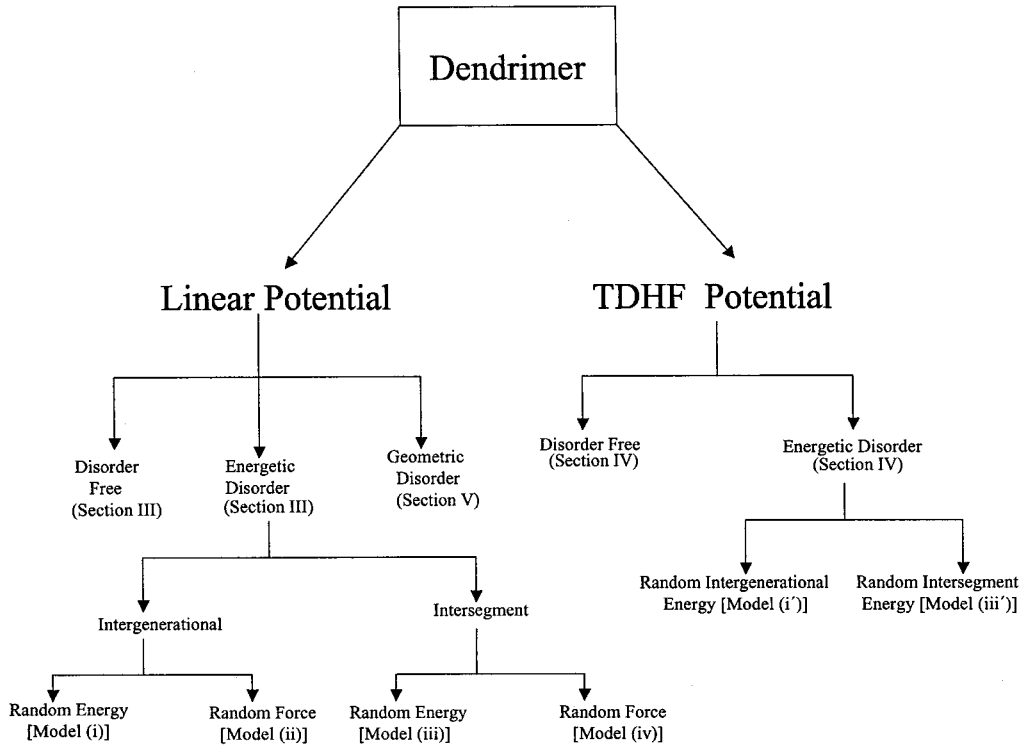

considerable theoretical significance.

In a recent letter [12], we reported preliminary studies of the effects of nonlinear dependence of the excitonic energy and realistic quenched disorder on excitonic diffusion on Cayley-tree-like dendrimers. We further carried out analytic investigations of diffusion on a disordered Cayley tree with a linear potential. Our findings can be summarized as follows:

(i) Due to the nonlinear variation of the funneling potential with the generation, an optimal generation number $n^*(g)$ was found beyond which the nonlinear potential drastically diminishes the light-harvesting efficiency. Moreover, increasing of the trapping time by the disorder (by slowing down the exciton diffusion) will be more pronounced if the dendrimer crosses this optimal size. Hence, for dendrimers larger than the optimal size, even though the total photon absorbance will increase due to the increase in the number of peripheral light absorbing sites, the slower excitonic migration towards the active center will make the light-harvesting antenna less effective.

(ii) We investigated the diffusion on a Cayley tree in the presence of a linear potential and considered various types of disorder, depending on the correlations among the energy fluctuations. For a specific type of disorder [See model (iv)], we found a dynamic phase transition to a highly disordered phase where only a few paths dominate the exciton migration. This resembles the equilibrium replica symmetry breaking transition found in other random systems (e.g., directed polymers in random media).

The purpose of this paper is to elaborate on and extend the results reported in our previous study. We further report the numerical study of diffusion on a Cayley tree with a specific kind of geometric disorder obtained by adding a few random connections between various sites to the usual tree structure. This *small world* model was first introduced by Watts and Strogatz [13] for Euclidean lattices.

The organization of the paper is as follows. The mean first passage line (MFPT) for random walk is reviewed in Sec. II. In Sec. III we discuss diffusion on a random Cayley tree with a linear potential. The effect of nonlinear potential on the exciton migration is reported in Sec. IV. The small world model is studied in Sec. V. Finally, we conclude in Sec. VI with a summary of our results.

A flow chart (Table I) of the different models discussed in this paper is given in Table I. The various models will be explained later.

II. RANDOM WALKS AND THE MEAN FIRST PASSAGE TIME (MFPT)

The MFPT is a faithful measure of the trapping efficiency defined as the average time it takes for an exciton to diffuse from the periphery to the core, where it gets trapped [14]. Another quantity of interest related to the MFPT is the mean residence time (MRT), which is the average time spent on a site of the tree (branch of the dendrimer) [14,15]. Our theoretical effort focused on calculating the MFPT and the MRT for a continuous time random walk with exponential distribution of waiting times, which gives a master equation for the probability $P_n(t)$ of the exciton to be on site n at time t. If the energy depends only on n, the problem becomes effectively one dimensional for $P_n(t)$. The random walker on the nth site of the one-dimensional chain jumps to nearest sites with rates R_i (toward the reflecting point) and T_i (toward the

trap). The random walk is described by the master equation [15]

$$\frac{d\mathbf{P}(t)}{dt} = -A\mathbf{P}(t), \tag{1}$$

where $\mathbf{P}(t)$ denotes the probability vector and hence the survival probability $S(t)=\Sigma_1^g P_n(t)$. A is the tridiagonal transition matrix. Written explicitly in terms of the rates R and T,

$$\dot{P}_0(t) = T_1 P_1(t),$$

$$\dot{P}_1(t) = T_2 P_2(t) - (T_1+R_1)P_1(t),$$

$$\dot{P}_n(t) = T_{n+1}P_{n+1}(t) + R_{n-1}P_{n-1}(t) - (T_n+R_n)P_n(t) \quad (1<n<g),$$

$$\dot{P}_g(t) = R_{g-1}P_{g-1}(T) - T_g P_g(t). \tag{2}$$

The trap (P_0) is not included in Eq. (1), while reflecting boundary conditions are imposed at $n=g$.

The formal solution of Eq. (1) is

$$\mathbf{P}(t) = \exp(-At)\mathbf{P}(0), \tag{3}$$

where $\mathbf{P}(0)$ is the initial condition. $\mathbf{P}(0) = [0,0,0,\ldots,1,0,0,0,\ldots]^T$ for an excitation that starts in the nth generation. The MFPT is obtained by integrating the survival probabilities $P_n(t)$ over time

$$\tau(g) = \int_0^\infty \sum_{n=1}^{g} P_n(t)dt = \sum_{n=1}^{g}\int_0^\infty P_n(t) \equiv \sum_{n=1}^{g} t_n, \tag{4}$$

where t_n is the MRT for generation n. Using the general solution, Eq. (3) [15,16],

$$\int_0^\infty \mathbf{P}(t)dt = \int_0^\infty \exp(-At)\mathbf{P}(0)dt = A^{-1}\mathbf{P}(0). \tag{5}$$

Hence the MRT at site n is given by

$$t_n = \int_0^\infty P_n(t) = \sum_j A_{nj}^{-1} P_j(0). \tag{6}$$

For an excitation that starts at the highest (periphery) generation g, $P_j(0)=\delta_{jg}$ and the MRT is given by [6]

$$t_1 = \frac{1}{T_1}, \quad n=1, \tag{7}$$

$$t_n = \frac{1}{T_n} + \sum_{i=0}^{n-2}\left(\frac{1}{T_i}\right)\prod_{j=i+1}^{n-1}\xi_j, \quad 1<n\leqslant g, \tag{8}$$

where $\xi_n \equiv R_n/T_{n+1}$ is the detailed balance ratio. The MFPT is given by

$$\tau(g) = \sum_{n=1}^{g-1} t_n \tag{9}$$

$$= \sum_{m=1}^{g}\frac{1}{T_m} + \sum_{m=2}^{g-2}\sum_{i=0}^{m-2}\left(\frac{1}{T_i}\right)\prod_{j=i+1}^{m-1}\xi_j. \tag{10}$$

An explicit form of this equation is given in the Appendix. Hereafter, we assume $T_n=1$ and treat ξ_n as independent variables with $\xi_n = c\exp\{-\beta[\epsilon(n+1)-\epsilon(n)]\}$, where $c+1$ is the coordination number of the tree ($c=2$ in our case), $\epsilon(n)$ denotes the energy of the nth segment, and $\beta=(KT)^{-1}$ is the Boltzmann factor.

III. RANDOM WALK AND MFPT ON A DISORDERED CAYLEY TREE WITH A LINEAR FUNNEL

The linear funneling potential assumes the form

$$\overline{\epsilon}(n) = nF, \tag{11}$$

F being the potential difference. For this model $\xi_n=\xi_0 = c\exp(-\beta F)$. Equation (10) can be easily summed (see the Appendix for details) to yield for the MFPT,

$$\tau(g) = \begin{cases} \xi\dfrac{\xi^g-1}{(\xi-1)^2} - \dfrac{g}{\xi-1} & \text{for} \quad \xi\neq 1 \\ \dfrac{g(g+1)}{2} & \text{for} \quad \xi=1. \end{cases} \tag{12}$$

For large g ($\gg 1$), Eq. (12) shows three distinct behaviors.

(a) $\xi>1$: $\tau(g)\sim\exp(g\ln\xi)$ (exponential regime).
(b) $\xi<1$: $\tau(g)\sim g$ (linear regime).
(c) $\xi=1$: $\tau(g)\sim g^2$ (diffusive behavior).

Real dendrimers have energy fluctuations and quenched (slow) energy disorder plays an important role in the energy transfer dynamics [17]. We have studied the effects of disorder on diffusion in the presence of a linear potential by considering four models of disorder denoted by (i)–(iv). These will be described below.

A. Intergenerational quenched disorder

Assuming that energy fluctuations in the segment lengths of the same generation are identical, the diffusion is mapped into an effective one-dimensional problem. We denote this type of disorder intergenerational.

Intergenerational energy fluctuations can be introduced in two ways. In the absence of correlations, we obtain the standard diagonal disorder (random-energy) model (i), where a random part ϵ_n is added to the linear energy $\overline{\epsilon}(n)$. In the second form of disorder [random force model (ii)], the energy differences $\Delta\epsilon_n$ $[=\epsilon(n+1)-\epsilon(n)]$ are treated as random variables with the positive average values $\overline{\epsilon}(n)$ to ensure funneling. Both models are one dimensional and the MFPT is given by Eq. (10).

1. Model (i): Random intergenerational energy

In this model, all segments in a given generation have the same random energy. Generational energies are made random by adding a fluctuating part ϵ_n to the linear potential

$$\epsilon(n)=\overline{\epsilon}(n)+\epsilon_n .$$

ϵ_n's are independent and identically distributed with the average $\langle \epsilon_n\rangle=0$ and $\overline{\epsilon}(n)$ is the linear potential defined in Eq. (11). A similar random-energy model has been considered previously [18] for a discrete random walk.

Hereafter $\langle\rangle$ will denote the average over disorder. We define $\eta_n=\exp(-\beta\epsilon_n)$ and assume $\langle \eta^{\pm 1}\rangle$ and $\langle \eta^{\pm 2}\rangle$ to be finite. The subscript n in $\langle \eta\rangle$ is omitted because the random variables ϵ_n's are independent and identically distributed. Hence

$$\xi_n\xi_{n-1}\cdots\xi_2\xi_1=c\exp[-\beta\{\epsilon(n+1)-\epsilon(n)\}]c\exp[-\beta\{\epsilon(n)-\epsilon(n-1)\}]\cdots c\exp[-\beta\{\epsilon(3)-\epsilon(2)\}]c \times\exp[-\beta\{\epsilon(2)-\epsilon(1)\}] \tag{13}$$

$$=\xi_0^n\{\exp[-\beta(\epsilon_{n+1}-\epsilon_n)]\}. \tag{14}$$

Averaging over realizations of disorder gives

$$\langle \xi_n\xi_{n-1}\cdots\xi_2\xi_1\rangle=\langle \eta\rangle\langle \eta^{-1}\rangle\xi_o^n. \tag{15}$$

Substituting this in Eq. (10) gives for the MFPT

$$\langle \tau(g)\rangle\sim\langle \eta\rangle\langle \eta^{-1}\rangle\tau_0(g), \tag{16}$$

where $\tau_0(g)$ is the MFPT [see Eq. (12)] for a linear potential with no disorder.

Similar to the ordered case, the disorder-averaged MFPT has three distinct regimes: linear ($\xi_0<1$), quadratic ($\xi_0=1$), and exponential ($\xi_0>1$) depending on the value of ξ_0. Even though the g dependence and the critical point ($\xi_0=1$) of the MFPT do not change by disorder, the magnitude of the disorder-averaged MFPT exceeds the corresponding value for the ordered system. Disorder slows down the first passage diffusion. If the fluctuating part of the energy ϵ_n has a Gaussian probability distribution $P_G(\epsilon)=(1/\sqrt{2\pi}\lambda)\exp\{-\epsilon^2/2\lambda^2\}$, then

$$\langle \tau_g\rangle\sim\langle \eta\rangle\langle \eta^{-1}\rangle\tau_0(g) =\langle\exp(-\beta\epsilon_n)\rangle\langle\exp(\beta\epsilon_n)\rangle\tau_0(g) =\exp(\beta^2\lambda^2)\tau_0(g). \tag{17}$$

The average MFPT is thus increased by the disorder-dependent factor of $\exp(\beta^2\lambda^2)$.

So far we have considered only the average MFPT, but due to disorder there will be fluctuations in the MFPT corresponding to various realizations of disorder. The distribution of MFPT due to disorder may be directly observed in single molecule spectroscopy [19]. We have calculated the rms fluctuations in the MFPT, $\langle(\Delta\tau)^2\rangle=\langle(\tau-\langle\tau\rangle)^2\rangle$ in different regimes of $\langle\tau(g)\rangle$.

In the linear regime ($\xi_0<1$), only the terms linear in ξ in Eq. (10) are sufficient to yield the correct scaling (in terms of g) for both $\langle\tau(g)\rangle$ and $\langle\Delta\tau^2\rangle$. Considering only the linear terms in Eq. (10), we get

$$\tau(g)\approx\{1\}+\{\xi_0\exp[-\beta(\epsilon_2-\epsilon_1)]+1\} +\{\xi_0\exp[-\beta(\epsilon_3-\epsilon_2)]+1\}+\cdots +\{\xi_0\exp[-\beta(\epsilon_g-\epsilon_{g-1})]+1\} =\xi_0\{\exp(-\beta\epsilon_2)\exp(\beta\epsilon_1)+\exp(-\beta\epsilon_3)\exp(\beta\epsilon_2) +\cdots+\exp(-\beta\epsilon_g)\exp(\beta\epsilon_{g-1})\}+g. \tag{18}$$

Averaging over realizations of disorder gives

$$\langle\tau(g)\rangle=(g-1)\xi_0\langle\eta\rangle\langle\eta^{-1}\rangle+g. \tag{19}$$

To calculate the fluctuation of the MFPT around its average we need $\langle[\tau(g)]^2\rangle$. Taking the disorder average of the square of Eq. (19),

$$\langle[\tau(g)]^2\rangle=(g-1)\xi_0^2\langle\eta\rangle^2\langle\eta^{-2}\rangle+2(g-1)\xi_0^2\langle\eta\rangle\langle\eta^{-1}\rangle +2\left\{\binom{g-1}{2}-(g-2)\right\}\xi_0^2\langle\eta\rangle^2\langle\eta^{-1}\rangle^2 +2g(g-1)\xi_0\langle\eta\rangle\langle\eta^{-1}\rangle+g^2. \tag{20}$$

From the average MFPT Eq. (19),

$$\langle[\tau(g)]\rangle^2=(g-1)^2\xi_0^2\langle\eta\rangle^2\langle\eta^{-1}\rangle^2+2g(g-1)\xi_0\langle\eta\rangle\langle\eta^{-1}\rangle +g^2. \tag{21}$$

Combining Eqs. (20) and (21) we obtain for the fluctuation in the MFPT,

$$\langle[\Delta\tau(g)]^2\rangle=\langle[\tau(g)]^2\rangle-\langle[\tau(g)]\rangle^2 =g\xi_0^2\{\langle\eta^2\rangle\langle\eta^{-2}\rangle+2\langle\eta\rangle\langle\eta^{-1}\rangle -3\langle\eta\rangle^2\langle\eta^{-1}\rangle^2\}. \tag{22}$$

Hence the relative fluctuation in the linear regime ($\xi_0<1$) will be given by

$$\frac{\Delta\tau}{\tau}=\frac{\langle(\Delta\tau(g))^2\rangle^{1/2}}{\langle\tau(g)\rangle}$$
$$\simeq\frac{\sqrt{g}\xi_0\{\langle\eta^2\rangle\langle\eta^{-2}\rangle+2\langle\eta\rangle\langle\eta^{-1}\rangle-3\langle\eta\rangle^2\langle\eta^{-1}\rangle^2\}^{1/2}}{g\{1+\xi_o\langle\eta\rangle\langle\eta^{-1}\rangle\}}$$
$$\sim\frac{1}{\sqrt{g}}. \tag{23}$$

In the previous calculation, only the terms linear in ξ were kept in order to obtain the fluctuation around the average in the linear regime. The same calculation in the exponential regime, which will be considered next, only involves the term containing the highest product of ξ's in Eq. (10). At the transition point $\xi_0=1$, proceeding along the same lines for the linear case but keeping all the terms of $\tau(g)$ in Eq. (10) and putting $\xi_0=1$ at the end yields $\delta\tau/\tau\simeq 1/\sqrt{g}$. The same scaling was found above in the linear regime.

In the exponential regime ($\xi_0>1$), the MFPT is dominated by the single term in expression (10). In this case

$$\tau(g)\simeq\xi_{g-1}\xi_{g-2}\cdots\xi_2\xi_1.$$

The average MFPT is then $\langle\tau(g)\rangle\simeq\xi_0^g\langle\eta\rangle\langle\eta^{-1}\rangle$ for large g, as expected. In this approximation $\langle[\tau(g)]^2\rangle\simeq\xi_0^{2g}\langle\eta^2\rangle\langle\eta^{-2}\rangle$, and the fluctuation in the MFPT is

$$\frac{\Delta\tau}{\tau}\simeq\left[\frac{\langle\eta^2\rangle\langle\eta^{-2}\rangle}{(\langle\eta\rangle\langle\eta^{-1}\rangle)^2}-1\right]^{1/2}, \tag{24}$$

which is a constant independent of g.

2. Model (ii): Random intergenerational force

In this model energy differences between consecutive generations are randomly distributed, but again all segments in the same generation are identical. Fluctuations of the energy levels are correlated and the energy differences $\Delta\epsilon_n$ are assumed to be identically distributed according to some probability distribution $P(\Delta\epsilon_n)$. This diffusion model was studied extensively in various contexts and was reviewed in [22]. The effect of disorder is more pronounced in this case compared with the random-energy model. The average MFPT is given by

$$\langle\tau(g)\rangle=\langle\xi\rangle\frac{\langle\xi\rangle^g-1}{(\langle\xi\rangle-1)^2}-\frac{g}{\langle\xi\rangle-1}. \tag{25}$$

$\langle\tau(g)\rangle$ again has three regimes, but the transition occurs at $\langle\xi\rangle=1$. Note that in model (i), this condition was $\xi_0=1$, and disorder did not change the transition point. In the present model, however, the transition point is shifted due to the stronger effect of disorder. In some regimes of the MFPT, the effect of disorder is so strong that the typical diffusion time differs from the MFPT. This indicates a broad distribution of the MFPT where the average is affected by the rare configurations with long first passage time. The more representative "typical" diffusion time is calculated as $\tau_{typ}=\exp\langle\ln\tau(g)\rangle$. Following [20], we define different scaling regimes of the MFPT and τ_{typ}.

(a) $\langle\xi\rangle<1$: $\langle\tau(g)\rangle$ is linear in g. $\langle\xi^2\rangle$ determines the fluctuation around the average. $\langle\tau^2(g)\rangle\sim g^2$ as long as $\langle\xi^2\rangle<1$ and hence the relative fluctuation $\delta\tau/\tau$ goes to a constant (similar to the random-energy case). For $\langle\xi^2\rangle>1$, however, $\langle\tau^2(g)\rangle$ grows exponentially with g as the typical behavior starts to differ from the MFPT. If $\langle\xi\rangle>1$, $\langle\tau(g)\rangle$ is always exponential in g. However, τ_{typ} varies depending on the value of $\langle\ln\xi\rangle$ (whether less than, equal to, or greater than 1).

(b) $\langle\xi\rangle>1$, $\langle\ln\xi\rangle<0$: The typical first passage time $[\tau_{typ}(g)=\exp\langle\ln\tau(g)\rangle]$ does not follow the average exponential behavior, but rather grows like a power law g^α with $\alpha=\langle\delta(\ln\xi)^2\rangle/2\langle\ln\xi\rangle$. For a Gaussian probability distribution $P_G(\Delta\epsilon)$ the above formula yields $\alpha=\beta^2\lambda^2/2(\ln\xi_0)$.

(c) $\langle\xi\rangle>1$, $\langle\ln\xi\rangle=0$ [21]: At this transition point (the "Sinai point"), $\langle\tau(g)\rangle$ is exponential in g, but the more representative $\tau_{typ}(g)$ is only exponential in $\sqrt{g}$ [22].

(d) $\langle\xi\rangle>1$, $\langle\ln\xi\rangle>0$: In this regime, both $\langle\tau(g)\rangle$ and $\tau_{typ}(g)$ diverge exponentially with g.

B. Intersegment quenched disorder

When energy fluctuations exist within the same generation (intersegment disorder), the system can no longer be mapped into a one-dimensional model and we have to use Eqs. (4) and (6) to compute the MFPT for the actual tree structure. The energy of site q_n is denoted $\epsilon_q(n)$. The random variables ξ_n's become matrices $\xi_n^{p,q}$, where (p,q) represents qth point of the nth generation and the pth point of the $(n+1)$th generation. (note that c is not included in this definition.) The detailed balance ratio becomes $\xi_n^{p,q}=\exp[-\beta\Delta\epsilon_{pq}(n)]=\xi\exp[-\beta(\epsilon_{p_{n+1}}-\epsilon_{q_n})]$, where ϵ_{q_n} is the fluctuating part of the energy and $\xi=\exp(-\beta[\overline{\epsilon}(n+1)-\overline{\epsilon}(n)])$ (so $\xi_0=c\xi$). From now on we assume that the branching ratio $c=2$. The MFPT for a particle released at the peripheral site 1_g of the g-generational tree is

$$\begin{aligned}\langle\tau^{1_g}(g)\rangle=&\{1\}+\{(\xi_1^{1,1}+\xi_1^{1,2})+1\}+\{\xi_1^{1,1}(\xi_2^{1,1}+\xi_2^{1,2})\\&+\xi_1^{1,1}(\xi_2^{2,3}+\xi_2^{2,4})+(\xi_2^{1,1}+\xi_2^{1,2})+1\}+\cdots\\&+\{\xi_1^{1,1}(\xi_2^{1,1}(\cdots(\,)\cdots)+\xi_2^{1,2}(\cdots(\,)\cdots))\\&+\xi_1^{1,2}(\xi_2^{2,3}(\cdots(\,)\cdots)+\xi_2^{2,4}(\cdots(\,)\cdots))+\cdots\\&+(\xi_{g-1}^{1,1}+\xi_{g-1}^{1,2})+1\}.\end{aligned} \tag{26}$$

We define the initial site average MFPT (ISA-MFPT) as

$$\overline{\tau(g)}=\frac{1}{N_g}\sum_{i_g=1}^{N_g}\tau^{i_g(g)}, \tag{27}$$

where $N_g=(1+c)c^{g-1}$ is the number of peripheral sites (leaves of the tree).

$\overline{\tau(g)}$ may be expressed again [see Eq. (9)] as a sum over ISA-MRT,

$$\overline{\tau(g)} = \sum_{n=1}^{g} \overline{t_n}. \tag{28}$$

Each of the $\overline{t_n}$ is made of a sum of products over ξ's up to generation n. Formally it may be expressed as

$$\overline{t_n} = 1 + \sum_{k=1}^{n-1} \left\{ \frac{1}{c^{k-1}} \sum_{i_k=1}^{c^{k-1}} T_{i_k}^{n} \right\}, \tag{29}$$

where $T_{i_k}^{n}$ stands for the contribution to $\overline{t_n}$ from a subtree rooted at site i_k in generation k and spreading out to the nth generation. This contribution is made of products of $(n-k)$ ξ's along the c^{n-k} paths going from the site i_k to the c^{n-k} different sites in generation n. The kth generation has c^{k-1} rooted subtrees with $i_k = 1, \ldots, c^{k-1}$. The contributions from subtrees rooted at the same generation are independent of each other. Symbolically,

$$T_{i_k}^{n} = \sum_{\Gamma_m} \left(\prod_{pq_m \in \Gamma_m} \xi_m^{p,q} \right) = \sum_{\Gamma_m} \exp\left[-\beta \sum_{pq_m} \Delta \epsilon_{pq}(m) \right], \tag{30}$$

where Γ_m are all paths on this subtree from i_k to generation n.

1. Model (iii): Random intersegment energy

In a fully disordered tree all segment energies (ϵ_{i_n}) are random and uncorrelated. The techniques applied in model (i) can be simply extended to this case with almost identical results (Fig. 2 shows the average MFPT for both the models).

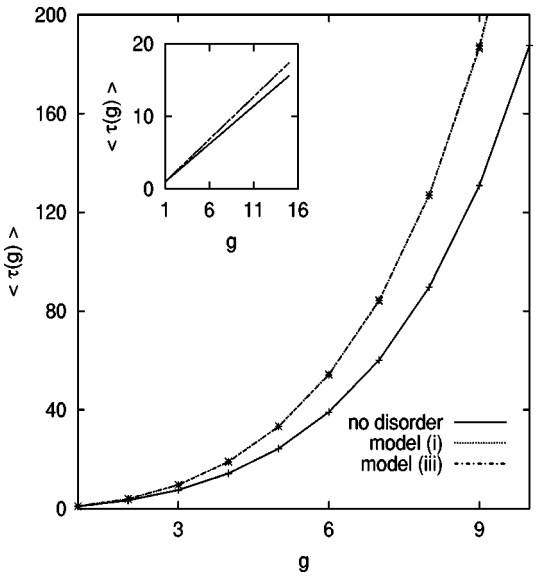

FIG. 2. The MFPT for the linear potential with both types of random-energy fluctuations (indistinguishable from each other) compared to that of the pure system (in the exponential regime). Inset: the same in the linear regime.

In the linear regime, the MFPT expression can be approximated by neglecting terms of order ξ^2 and higher. For $c=2$ we have

$$\begin{aligned}
\tau^{1_g}(g) \approx & \{1\} + \{\xi \exp[-\beta(\epsilon_{1_2} - \epsilon_{1_1})] + \xi \exp[-\beta(\epsilon_{1_2} - \epsilon_{1_1})] + 1\} + \{\xi \exp[-\beta(\epsilon_{1_3} - \epsilon_{1_2})] + \xi \exp[-\beta(\epsilon_{2_3} - \epsilon_{1_2})] + 1\} \\
& + \cdots + \{\xi \exp[-\beta(\epsilon_{1_g} - \epsilon_{1_{g-1}})] + \xi \exp[-\beta(\epsilon_{2_g} - \epsilon_{1_{g-1}})] + 1\} \\
= & \xi\{\exp[-\beta(\epsilon_{1_2} - \epsilon_{1_1})] + \exp[-\beta(\epsilon_{1_2} - \epsilon_{1_1})] f + \exp[-\beta(\epsilon_{1_3} - \epsilon_{1_2})] + \exp[-\beta(\epsilon_{2_3} - \epsilon_{1_2})] + \cdots \\
& + \exp[-\beta(\epsilon_{1_g} - \epsilon_{1_{g-1}})] + \exp[-\beta(\epsilon_{2_g} - \epsilon_{1_{g-1}})]\} + g.
\end{aligned} \tag{31}$$

Upon averaging over realizations of disorder we obtain

$$\begin{aligned}
\langle \tau^{1_g}(g) \rangle &= 2(g-1)\xi \langle \eta \rangle \langle \eta^{-1} \rangle + g \\
&= (g-1)\xi_0 \langle \eta \rangle \langle \eta^{-1} \rangle + g \quad \text{for large } g,
\end{aligned} \tag{32}$$

where $\xi_0 = 2\xi$ with $c=2$.

The average MFPT is identical for models (i) and (iii). The fluctuation of the MFPT around its average is connected to $\langle [\tau(g)]^2 \rangle$. Taking the disorder average of the square of Eq. (31)

$$\begin{aligned}
\langle [\tau(g)]^2 \rangle = & 2(g-1)\xi^2 \langle \eta^2 \rangle \langle \eta^{-2} \rangle + 2(g-1)\xi^2 \langle \eta \rangle^2 \langle \eta^{-2} \rangle \\
& + 2\{2(g-1)\}\xi^2 \langle \eta \rangle \langle \eta^{-1} \rangle + 2\left\{ \binom{2(g-1)}{2} \right. \\
& \left. - (g-1) - 2(g-2) \right\} \xi^2 \langle \eta \rangle^2 \langle \eta^{-1} \rangle^2 \\
& + 2\{2g(g-1)\}\xi \langle \eta \rangle \langle \eta^{-1} \rangle + g^2.
\end{aligned} \tag{33}$$

The average MFPT equation (32) yields

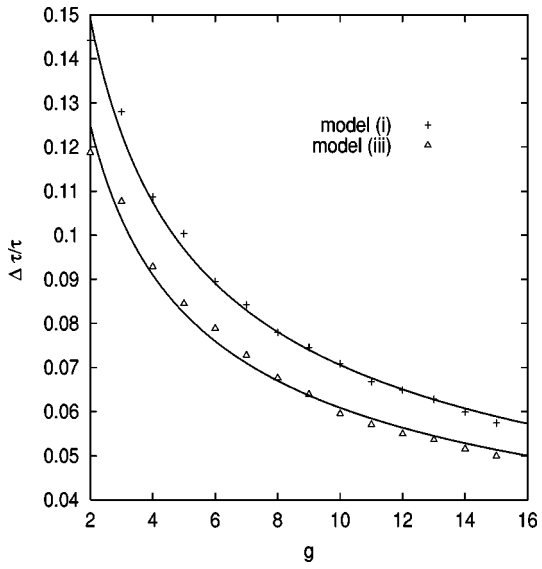

FIG. 3. The relative fluctuation in the MFPT for both types of random-energy disorder (intergenerational and intersegment) with a linear potential (in the linear regime).

$$\langle[\tau(g)]\rangle^2 = 4(g-1)^2\xi^2\langle\eta\rangle^2\langle\eta^{-1}\rangle^2 + 4g(g-1)\xi\langle\eta\rangle\langle\eta^{-1}\rangle + g^2 = (g-1)^2\xi_0^2\langle\eta\rangle^2\langle\eta^{-1}\rangle^2 + 2g(g-1)\xi_0\langle\eta\rangle\langle\eta^{-1}\rangle + g^2. \quad (34)$$

Equations (33) and (34) yield for the fluctuation in the MFPT

$$\langle[\Delta\tau(g)]^2\rangle = \langle[\tau(g)]^2\rangle - \langle[\tau(g)]\rangle^2 = g\xi_0^2\left\{\frac{1}{2}\langle\eta^2\rangle\langle\eta^{-2}\rangle + \frac{1}{2}\langle\eta\rangle^2\langle\eta^{-2}\rangle + \langle\eta\rangle\langle\eta^{-1}\rangle - 2\langle\eta\rangle^2\langle\eta^{-1}\rangle^2\right\}. \quad (35)$$

The relative fluctuation $\Delta\tau/\tau \sim 1/\sqrt{g}$ scales with g the same way as in the case of intergenerational disorder, but the amplitude is smaller in this model. This can be seen by comparing Eqs. (22) and (35) and using $\langle\eta\rangle^2 \leqslant \langle\eta^2\rangle$. This is also verified by our numerical calculation (Fig. 3) where we have kept all the terms in the MFPT expression. In the exponential regime, the relative fluctuations $\Delta\tau/\tau$ will still saturate to a g-independent value, but the latter will be also smaller than that reached with model (i).

The differences between models (i) and (iii) may also stem from the additional fluctuations in the MFPT for the latter model, which arise from distinct initial sites at the periphery. For initial excitations starting at two different peripheral sites (on the same dendrimer) separated by an ultrametric distance p, the fluctuations in the MFPT is given by

$$\langle[\Delta\tau(g)]^2\rangle \sim p.$$

This is not surprising because the two excitons starting from two different sites separated by an ultrametric distance p have to move p segments before they can be on the same path. Hence p is the only relevant length scale for the fluctuation in $\tau(g)$ mentioned above. Averaging over all possible peripheral sites, the fluctuation scales with g the same way as the dendrimer-to-dendrimer fluctuations discussed above. The amplitude of the fluctuation is different from that of the dendrimer-to-dendrimer fluctuations and depends heavily on the branching ratio c of the tree.

2. Model (iv): Random intersegment force

This model assumes that all energy differences $[\Delta\epsilon_{pq}(n) \equiv \epsilon_p(n+1) - \epsilon_q(n)]$ between neighboring segments are random. We observe a new transition apart from the usual linear to exponential regime transition of the MFPT. This is a one-step replica symmetry breaking transition from a weakly disordered (high-temperature) phase to a highly disordered (low-temperature) phase. In the weakly disordered phase all paths contribute to $\overline{\tau(g)}$, whereas in the highly disordered phase $\overline{\tau(g)}$ is dominated by a few paths. Similar dynamic transition was predicted [23] for kinetic pathways in protein folding.

This transition occurs only in this model. It cannot occur in models (i) and (ii) since in these models there is effectively a single pathway from the periphery to the center (i.e., all pathways are equivalent). It cannot occur in model (iii) since the random-energy effect is very limited. For any path, independent of its length, only the random energies at the initial and final sites are contributing. This is insufficient to cause an energetic disparity that will overcome the entropic advantage of having maximum number of paths contributing.

In the low-temperature phase the distribution of $\xi_n^{p,q} = \exp[-\beta\Delta\epsilon_{p,q}(n)]$ becomes very broad. The important contributions will come from those paths for which $\Sigma_{(pq)_n}\Delta\epsilon_{p,q}(n)$ is large and negative. We also assume that the constant force $\overline{\epsilon} = \epsilon_o$ is weak and the system is in the exponential regime. The linear regime will be discussed later. We thus focus on the large ξ regime (it is sufficient for them to be typically larger than $1/c$). In this regime, the largest contributions will come from the longest paths, and if a qualitative change in the behavior will occur it will be noticeable first in the dominant contribution from the largest of all subtrees. We will thus look for a new behavior in the ISA-MRT by examining the maximal tree rooted at $k=1$. The same argument may be repeated while looking at $\overline{\tau(g)}$: its dominant contribution in this regime will come from $\overline{t_g}$, namely, the ISA-MRT on the most extremal generation with $n=g$.

Searching for a possible abrupt change in the properties of ISA-MFPT, we will therefore examine the largest tree contributing to $\overline{t_g} \sim T_1^g$ since it has the largest energy disparity. As long as its behavior is normal, so will be all other terms. Once its behavior changes, it will affect that of $\overline{t_g}$ and then that of $\overline{\tau(g)}$, to which it makes the largest contribution.

The contribution of T_1^g is akin to a partition function of a so-called ''random-directed polymer'' on a Cayley tree,

which is known to have a glass transition (in the thermodynamic limit). Physically the transition is between a high-temperature phase $T \geqslant T_g$ at which all paths contribute, while for $T \leqslant T_g$ only a finite number of them do. The transition is of one-step replica symmetry breaking (1RSB) type. The $n \to 0$ replica trick was used to study its transition point. A complete analysis using this trick is available [11]. Here we present a simpler, more intuitive outline. In the very-high-temperature regime it may be shown that all moments of the MFPT (or the ''partition function,'' in the polymer picture) obey $\langle T^k \rangle = \langle T \rangle^k$. Hence, in the large-$T$ limit, all thermodynamic properties of the quenched system are given by those in which the disorder is annealed. In this regime $\langle T_1^g \rangle$ is easily computed and found to be

$$\langle T_1^g \rangle = [c \langle \exp(-\beta \Delta \epsilon) \rangle]^g. \tag{36}$$

For large g we have

$$\langle T_1^g \rangle = [\exp\{-\beta f\}]^g, \tag{37}$$

where $f(\beta) = -(1/\beta) \ln \langle T_1^g \rangle$ is the free energy per generation.

When the random-energy difference $\Delta \epsilon$ follows a Gaussian distribution $P_G(\Delta \epsilon) = (1/\sqrt{2\pi}\lambda) \exp[-(\Delta \epsilon - \epsilon_0)^2 / 2\lambda^2]$, the free energy is given by

$$\beta f = \beta \epsilon_0 - \ln c - \frac{1}{2} \beta^2 \lambda^2.$$

The transition point can be determined by the vanishing point of the entropy $S(= -\partial f / \partial T = \ln c - \lambda^2 / 2T^2$, where we assumed $K_B = 1$). This yields $\beta_g = \sqrt{2 \ln c}/\lambda$, which is the transition temperature from the weakly disordered to the highly disordered phase.

For low temperatures $\beta > \beta_g$ the entropy remains zero. This is achieved [11] by expressing the free energy as $f = \epsilon_0 - \ln c / m\beta - m\beta\lambda^2/2$, and $m \in [0,1]$ is chosen such that f is maximal. For $\beta < \beta_g$, $m = 1$ and the previous result holds. For $\beta > \beta_g$, $\partial f / \partial m = 0$ (which implies $\partial f / \partial T = 0$) yields

$$m = \frac{\sqrt{2 \ln c}}{\beta \lambda} = \frac{\beta_g}{\beta} < 1. \tag{38}$$

For a general distribution the requirement is to maximize

$$f(m) = -\frac{1}{m\beta} [\ln c + \ln \langle \exp(-m\beta \Delta \epsilon) \rangle].$$

The physical meaning of m is explained by the existence of a finite (in the thermodynamic $g \to \infty$ limit) number of paths that contribute to T_1^g, and therefore to $\overline{t_g}$ and $\overline{\tau(g)}$ as well. To see that, we need to define the overlap q between the contribution of two different products (paths) in the sum [and its distribution $P(q)$], which plays here the role of an order parameter. It is defined as the weighted (over all paths) fraction of the way the two paths will go together on the same segments, averaged over the disorder. At high temperatures all paths are essentially equivalent and the probability for any overlap vanishes. At $T = 0$ there is a single dominant path with the minimal energy (the ''ground state'') that makes the only contribution and thus both paths will overlap all the way giving $q = 1$ with probability 1. It was shown [11] that for this system the only two possible overlaps are $q = 0$ and $q = 1$. Their respective probabilities, however, change in the glassy phase and are given by

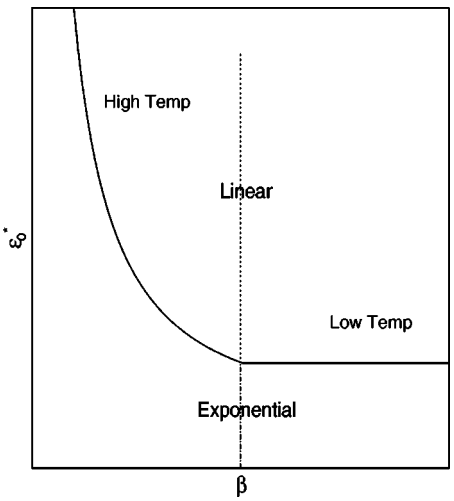

FIG. 4. The (ϵ_0, T) phase diagram for the replica symmetry breaking transition.

$$P(q) = \delta(q) \quad \text{for} \quad \beta < \beta_g \quad \text{and}$$

$$P(q) = m\,\delta(q) + (1-m)\,\delta(q-1) \quad \text{for} \quad \beta > \beta_g, \tag{39}$$

where $m = T/T_g$ was introduced before.

So far the discussion was limited to the exponential regime. Increasing ϵ_o will lead to the transition into a linear regime at $\epsilon_o = \epsilon_o^*(\beta)$. For $\beta < \beta_g$ the transition is given by the expected ''annealed'' condition $c\langle \xi \rangle = 1$, which yields $\epsilon_o^* = \ln c/\beta + \frac{1}{2}\beta\lambda^2$. For $\beta > \beta_g$, in the glassy phase free energy is given by

$$f(m,\beta) = \frac{\ln c}{m\beta} + \frac{m\beta\lambda^2}{2}. \tag{40}$$

Since $m\beta = \beta_g$ the critical force remains constant within the glassy phase for $T_g < T < 0$ and is equal to its value at the transition point $(\beta = \beta_g)$, which is given by

$$\epsilon_0^*(\beta > \beta_g) = \frac{\ln c \lambda}{\sqrt{2 \ln c}} + \frac{\sqrt{2 \ln c}\lambda}{2} = \lambda \sqrt{2 \ln c}. \tag{41}$$

The expected (ϵ_o, T) phase diagram is shown in Fig. 4

We should also note that crossing β_g within the linear regime yields only a glassy crossover and not a sharp transition. This is due to the fact that the ISA-MRT converges to a finite value even as $g \to \infty$. The longer paths thus make an exponentially small (in their length) contribution, the system is dominated by paths of finite length and the ''glass transition'' takes place in an effectively finite system.

IV. MFPT FOR THE NONLINEAR TIME-DEPENDENT HARTREE-FOCK POTENTIAL

In the preceding section the funneling energy was assumed to vary linearly with the generation number n $(=0,1,2,\ldots,g)$. However, electronic structure calculations by Tretiak, Chernyak, and Mukamel [24] show a strong nonlinear dependence of the exciton energy (on n).

The funneling effect of extended dendrimers originates from the variation of the segment lengths. We denote by n $(=1,2,\ldots,g)$ the nth generation starting from the center. The peripheral $n=g$ generation is made from the $m=1$ monomer. The number of monomers increases by one going from one generation to the next towards to the center. The number of acetylene monomers in the nth generation is thus $l=g-(n-1)$. The n dependence of the excitation energy was computed using the time-dependent Hartree-Fock (TDHF) technique and fitted to the form [25]

$$\epsilon(n)=A\left[1+\frac{L}{g-(n-1)}\right]^{0.5} \tag{42}$$

with $A=2.80\pm0.02$ (eV) and $L=0.669\pm0.034$.

A. Ordered dendrimer

Using Eq. (42), the detailed balance ratio becomes

$$\xi_n=c\exp-\frac{A}{kT}\left\{\left(1+\frac{L}{g-n}\right)^{0.5}-\left(1+\frac{L}{g-n+1}\right)^{0.5}\right\}. \tag{43}$$

The points of the same generation are identical and we can calculate the MRT and MFPT for this potential using the expressions (8) and (10) for one-dimensional random walk starting at the periphery. The mean time spent by an exciton in the nth generation is given by

$$t_n=\exp\left[-A\left\{1+\frac{L}{g-(n-1)}\right\}^{0.5}\right]\times\sum_{r=1}^{n}c^{(n-1)}\exp\left[A\left\{1+\frac{L}{g-(r-1)}\right\}^{0.5}\right]. \tag{44}$$

The total time to reach the trap will be sum of all the τ_n's, and the MFPT is

$$\tau(g)=\sum_{n=1}^{g}\tau_n=\sum_{n=1}^{g}\exp\left[-A\left\{1+\frac{L}{g-(n-1)}\right\}^{0.5}\right]\times\sum_{r=1}^{n}c^{(n-1)}\exp\left[A\left\{1+\frac{L}{g-(r-1)}\right\}^{0.5}\right]. \tag{45}$$

The above expression for $\tau(g)$ is plotted in Fig. 5 to show that the MFPT for this potential is quite different compared to that for the constant potential difference. We find that it depends linearly on g for the first few generations, but gradually changes to exponential with increasing g.

The behavior of the MFPT can be better understood in terms of MRT. The MRT is not a monotonic function of n, as

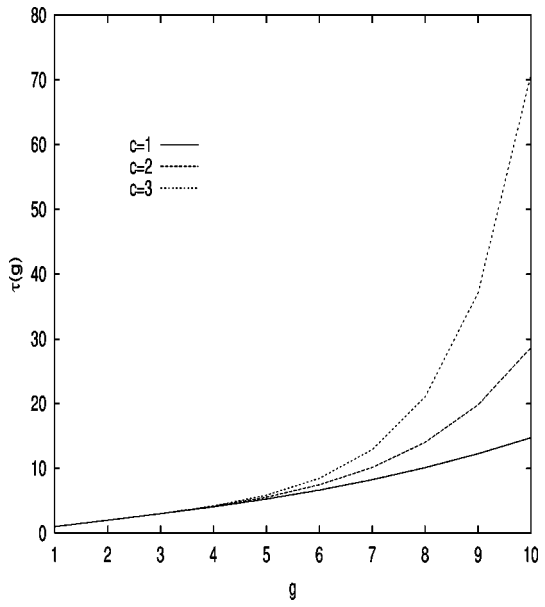

FIG. 5. The MFPT vs g for the ordered TDHF nonlinear potential for different branching ratios of the tree.

can be seen in Fig. 6 [plotted using the Eq. (44) of t_n] for the TDHF potential. At the generations near the periphery ($g-n\ll g$) the energy difference between generations is large and the funneling force is so strong that it overcomes the outward entropic force of $c\geqslant 2$. Near the center, on the other hand, the larger is g, the weaker is the funneling force and the entropic term dominates. The competing effects nearly cancel at some intermediate generation $n=n^*(g)$ where the exciton spends maximum time. For large g, an estimate for n^* may obtained from the recursion relation satisfied [from Eq. (8)] by the MRT's,

$$t_n=\xi_{n-1}t_{n-1}+1. \tag{46}$$

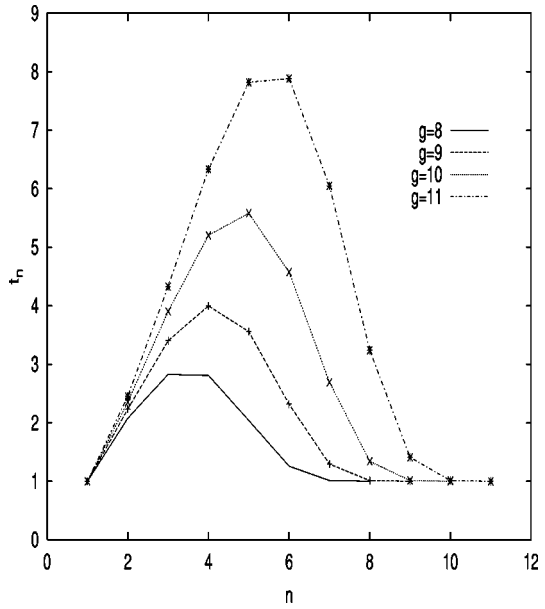

FIG. 6. The MRT vs n for the ordered TDHF potential for different values of g.

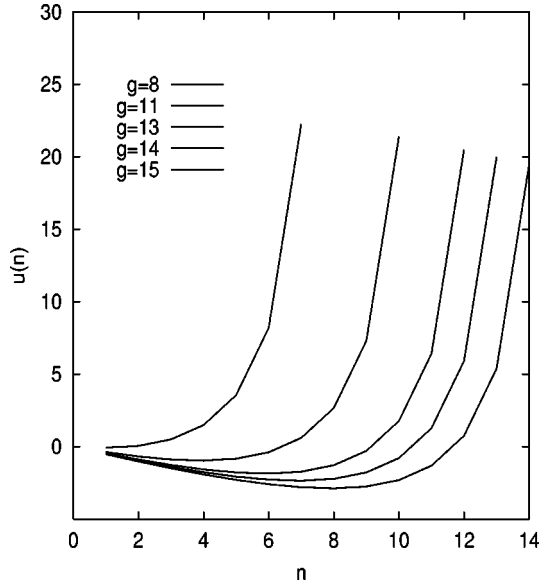

FIG. 7. The free energy $u(n)$ for the ordered TDHF nonlinear potential are plotted for different values of g.

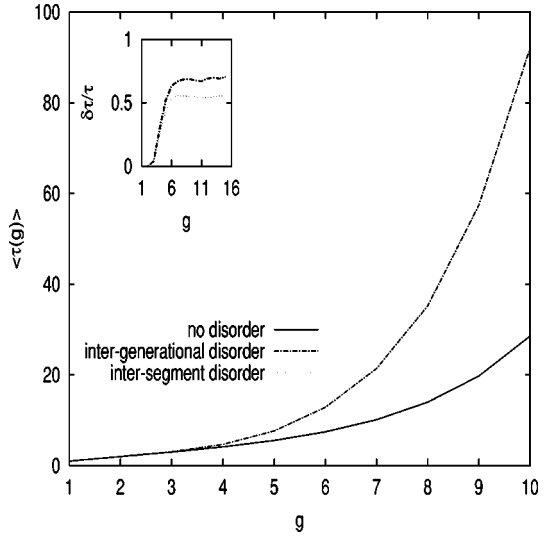

FIG. 8. The MFPT for the TDHF potential with both types of random energy (indiscernible from each other) compared to that of the pure system. Inset: their relative rms variations vs g.

For t_N to be maximal, $t_{n+1}/t_n=\xi_n+1/t_n<1$, hence $\xi_n<1$. Similarly requiring $\tau_n/\tau_{n-1}>1$ yields $\xi_{n-1}+1/\tau_{n-1}>1$, so for large τ_{n-1} (or equivalently large g) we may take $\xi_{n-1}\geqslant 1$. τ_n is therefore maximized as $\xi_n\to 1$ from below. Using expression (43) we obtain $n\sim(g-\kappa+1)$ where κ $[=\kappa(A,L,c)]$ is a constant (independent of n and g) and $n^*(g)$ is the closest integer. This formula works well for our system for $g\geqslant 12$ and holds approximately (off by only one generation) for $7\leqslant g<11$. Clearly, the larger the g, the better is the estimate of $n^*(g)$.

To understand the behavior of the MRT, the reduced free energy $u(n)=\beta\epsilon(n)-n\ln c$ is plotted in Fig. 7. The MRT is maximal at the site at which the free energy is minimum. For large g, both $n^*(g)$ and the energy difference between the center and n^* increases with g. As a result, the time to reach the center from n^* grows exponentially with g (the time to arrive at n^* from $n=g$ is always much shorter). If g is small enough, however, the values of n^* and $u(n^*)$ increase only weakly with g and the MFPT dependence on g may be approximated by a power series (dominated initially by the linear term).

For fixed g, the MFPT may be changed by variations of the coordination number c and the temperature T. Decreasing the temperature makes the funneling more effective. As a result, the crossover from the linear to the exponential regime occurs at a higher g. Increasing c has a similar effect: both the outbound ''entropic force,'' which competes with the energy funneling, and the MFPT increase (Fig. 5).

We have shown that for ordered dendrimers there exists a temperature and coordination number dependent specific size, below which the the MFPT is almost linear in g, whereas above it the MFPT starts to grow exponentially.

B. Random-energy fluctuations

We introduced disorder by adding a fluctuating part to the energy from an uniform probability distribution. The maximum value of the fluctuation is taken to be $\pm 4\%$ of the energy value. Similar to the random-energy models (i) and (iii) for the linear potential, intergenerational [model (i′)] and intersegment [model (iii′)] types of disorder were considered separately.

For the intergenerational random energy [model (i′)] we used the MFPT expression (10) obtained for a one-dimensional random walk. For the intersegment random energy [model (iii′)], the MFPT formula (26) for a Cayley tree can be used to calculate the time spent by an exciton in the nth generation starting from the point 1 (the points are labeled as $1,2,3,\ldots,2^{g-1}$) at the periphery,

$$t_n=\sum_{m=1}^{n}\left\{\exp[\beta\epsilon(m,1)]\sum_{r=1}^{n-m}\exp[-\beta\epsilon(n,r)]\right\}, \quad (47)$$

where $\epsilon(n,r)$ is energy of the rth branch of the nth generation of the tree. r can take values $1,2,3,\ldots,2^{n-1}$. The MFPT is obtained by summing all the t_n's. The effect of disorder was studied by numerically averaging the MFPT over different realizations of the disorder and is plotted in Fig. 8. This shows the disorder-averaged ($\sim 10^4$ realizations) MFPT for both intergenerational and intersegment disorders and also the case with no fluctuation. Disorder seems to work against the funneling and increases the MFPT. The effect of disorder is more pronounced in the exponential regime of the MFPT (Fig. 8). Hence, to achieve efficient funneling, dendrimers should not exceed the optimal size beyond which the nonlinear potential and the disorder make the excitons exponentially slow.

The disorder-averaged MFPT is identical for the intergenerational disorder model (i′) and the intersegment disorder model (iii′), consistent with our analytical calculation for models (i) and (iii). However the fluctuations around the average MFPT, $\delta\tau(g)$, are different (Fig. 8) especially for large

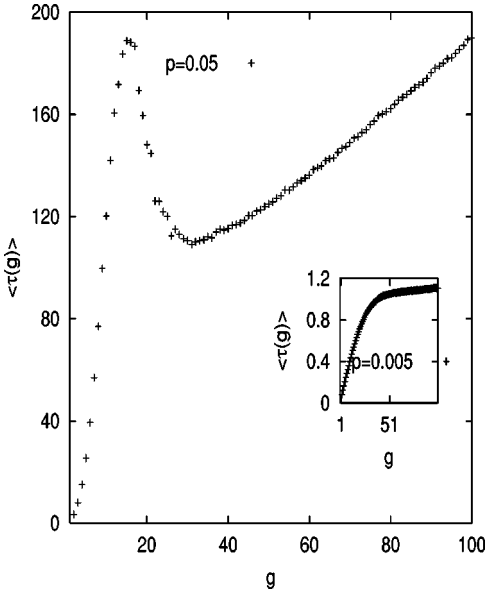

FIG. 9. The MFPT vs g for the small world model (exponential regime). Inset: the same for the linear regime.

g, and the relative fluctuation saturates to a larger value for the intergenerational disorder.

V. GEOMETRIC DISORDER: DIFFUSION ON A TREE WITH RANDOM CONNECTIONS

Different forms of generic networks have drawn much recent interest. The small world model was introduced by Watts and Strogatz [13] and received considerable attention in the past two years [26]. The model assumes a regular lattice and fixed number of nearest neighbor connections with a few randomly chosen connections between vertices. The essential features of this model are (i) high local connectivity that resembles a regular graph, (ii) the average distance between any two points scales as $\sim \ln L$, where L is the linear size of the graph. This is an important property of a random graph.

Inspired by this model we have studied the effect of a few random connections on the exciton diffusion. We first considered the MFPT for a one-dimensional chain with some random connections made between any two vertices with a fixed small probability. For a given chain length L, there exists a critical probability for random connections ($p_c \sim L^{1/d}$ [13]), above which the small world effects are observed. We have performed a numerical simulation of the MFPT for a one-dimensional small world chain using a generalized form of the master equation (1), where we allow few hoppings between vertices chosen randomly. We then averaged over different realizations of random connections. When $p > p_c$, we found that the average MFPT scales logarithmically (instead of linearly)with g (Fig. 9) for $\xi_0 < 1$. When $\xi_0 > 1$, the disorder-averaged MFPT grows almost linearly instead of exponentially with g (Fig. 9). This may be rationalized in terms of the average distance between any two vertices which is supposed to behave as $\ln g$, where g is the length of the system. Hence we can approximate a small world linear chain of length g by a regular linear chain of length $\ln g$. Then the average MFPT in a small world one-dimensional chain will be linear in $\ln g$ [i.e., $\tau(g) \sim \ln g$] for $\xi_0 < 1$. For $\xi_0 > 1$, the MFPT is exponential in $\ln g$ and hence $\tau(g) \sim \exp(\alpha \ln g) = g^{\alpha}$, where α is a constant. In our simulations $\alpha \sim 1$, so the MFPT grows linearly. As the probability p of random connections is decreased, the onset of the small world effect occurs at larger system sizes [26].

On a tree we add a few random connections between vertices of different generations. The resulting diffusion on such a ''small world tree'' yields results similar to the one-dimensional case. Disorder-averaged MFPT again shows logarithmic ($\xi_0 < 1$) or power-law ($\xi_0 > 1$) scaling with the number of generations g. Since only a few random connections can make the funneling much faster, it should be worthwhile to synthesize dendrimers with such shortcuts.

VI. CONCLUSIONS

We have investigated analytically the diffusion on a disordered Cayley tree in the presence of a linear potential. Fluctuations around the MFPT showed different forms of scaling (in terms of g) depending on the types of disorder and the scaling regime of MFPT. For a specific form of disorder (random intersegment force) we found a new dynamic transition in the MFPT. In the low-temperature (highly disordered) phase, the MFPT is dominated by a few paths. This transition resembles the one-step replica symmetry breaking glass transition found in other disordered systems like random-directed polymers.

We have also considered exciton diffusion on dendrimers with a nonlinear funneling energy. For dendrimers with a nonlinear potential larger than a specific size, even though the number of light-absorbing sites at the periphery increases, the MFPT starts to grow exponentially (with g), resulting in slow exciton trapping. Quenched disorder slows down the exciton diffusion towards the center. This effect is more pronounced when the MFPT of the corresponding ordered system is in the exponential regime. Hence to achieve an efficient funneling of excitons, the number of generations must be restricted to some optimal value. We have determined this optimal size for a particular class of phenylacetylene dendrimers. For large dendrimers, the free energy attains its minimum at $n^{\star}(g)$ where an exciton spends most of its time during its journey towards the center. Assuming a steady supply of long-lived photoexcitations, the excitons will start gathering at $n^{\star}(g)$, rendering the single-exciton picture invalid. In that case, we have to consider exciton-exciton interaction and annihilation processes [27].

Finally, we have considered diffusion on a lattice with a few random connections (''small world'') between any two vertices. The effect of random connections is to reduce the effective system size logarithmically. Numerical calculations show that the disorder-averaged MFPT is also decreased by a logarithmic factor. Hence there will be an exponential gain in the exciton trapping. This might have interesting consequences for information propagation through hierarchical social communication networks.

ACKNOWLEDGMENTS

This work was supported by the Chemical Sciences Division of the Office of Basic Energy Sciences of the DOE, Grant No. DE-FG02-01ER15155.

APPENDIX

The MFPT equation (10) can be expressed as

$$\tau(g)=\{1\}+\{\xi_1+1\}+\{\xi_2\xi_1+\xi_2+1\}+\cdots+\{\xi_n\xi_{n-1}\cdots\xi_2\xi_1+\xi_n\xi_{n-1}\cdots\xi_2+\cdots\xi_n\xi_{n-1}+\xi_n+1\}+\cdots+\{\xi_{g-1}\xi_{g-2}\cdots\xi_2\xi_1+\xi_{g-1}\xi_{g-2}\cdots\xi_2+\cdots\xi_{g-1}\xi_{g-2}+\xi_{g-1}+1\}, \tag{A1}$$

where $T_i=1$ is assumed.

For the linear potential the sum in Eq. (10) assumes the form

$$\tau(g)=\{1\}+\{\xi+1\}+\{\xi^2+\xi+1\}+\cdots+\{\xi^n+\xi^{n-1}+\cdots+\xi^2+\xi+1\}+\cdots+\{\xi^{g-1}+\xi^{g-2}+\cdots+\xi^2+\xi+1\}. \tag{A2}$$

This can be recast as

$$\tau(g)=g+(g-1)\xi+(g-2)\xi^2+\cdots 2\xi^{g-2}+\xi^{g-1}. \tag{A3}$$

This series can be summed to yield Eq. (12).

[1] R. Kopelman, M. Shortreed, Z. Shi, W. Tan, Z. Xu, J. Moore, A. Bar-Haim, and J. Klafter, Phys. Rev. Lett. **78**, 1239 (1997).

[2] D. A. Tomalia, A. M. Naylor, and W. A. Goddand, Angew. Chem. Int. Ed. Engl. **29**, 138 (1990).

[3] V. Blazani, S. Campagna, G. Denti, A. Juris, S. Serroni, and M. Venturi, Acc. Chem. Res. **31**, 26 (1998).

[4] J. Frechet, Science **263**, 1710 (1994).

[5] C. Devadoss, P. Bharathi, and J. S. Moore, J. Am. Chem. Soc. **118**, 9635 (1996); M. Shortreed, Z-Y. Shi, and R. Kopelman, Mol. Cryst. Liq. Cryst. Sci. Technol., Sect. **28**, 95 (1996); M. R. Shortreed, S. F. Swallen, Z-Y. Shi, W. Tan, Z. Xec, C. Devadoss, J. S. Moore, and R. Kopelman, J. Phys. Chem. B **101**, 6318 (1997).

[6] A. Bar-Haim, J. Klafter, and R. Kopelman, J. Am. Chem. Soc. **119**, 6197 (1997); A. Bar-Haim and J. Klafter, J. Phys. Chem. B **102**, 1662 (1998); J. Lumin. **76-77**, 197 (1998); J. Chem. Phys. **109**, 5187 (1998).

[7] C. W. Rella, A. Kwok, K. D. Rector, J. R. Hill, H. A. Schwettmann, D. D. Dlott, and M. D. Fayer; Phys. Rev. Lett. **77**, 1648 (1996).

[8] H. P. Lu and X. S. Xie, Nature (London) **385**, 143 (1997).

[9] M. Pope and C. E. Swenberg, *Electronic Processes in Organic Crystals*, 2nd ed. (Oxford University Press, Oxford, New York, 1999).

[10] B. D. Hughes, *Random Walks and Random Environments* (Oxford University Press, Inc., New York, 1995).

[11] B. Derrida, Phys. Rev. Lett. **45**, 79 (1980); B. Derrida and H. Spohn, J. Stat. Phys. **51**, 817 (1988); J. Cook and B. Derrida, J. Phys. A **23**, 1523 (1990); Y. Y. Goldschmidt, *ibid.* **31**, 9157 (1998).

[12] S. Raychaudhuri, Y. Shapir, V. Chernyak, and S. Mukamel, Phys. Rev. Lett. **85**, 282 (2000).

[13] D. J. Watts and S. H. Strogatz, Nature (London) **393**, 440 (1998).

[14] I. Oppenheim, K. E. Shuler, and G. H. Weiss, *Stochastic Processes in Chemical Physics* (MIT Press, Cambridge, MA, 1977).

[15] E. W. Montroll and K. E. Shuler, Adv. Chem. Phys. **1**, 361 (1958).

[16] N. G. Van Kampen, *Stochastic Processes in Physics and Chemistry* (North-Holland, Amsterdam, Holland, 1981).

[17] G. Weiss, Adv. Chem. Phys. **13**, 1 (1966).

[18] K. P. N. Murthy and K. W. Kehr, Phys. Rev. A **40**, 2082 (1989).

[19] W. E. Moerner and M. Orrit, Science **283**, 1670 (1999).

[20] J. P. Bouchaud and A. Georges, Phys. Rep. **195**, 127 (1990).

[21] Ya. G. Sinai, Russ. Math. Surveys **25**, 137 (1970).

[22] S. H. Noskowicz and I. Goldhirsch, Phys. Rev. Lett. **61**, 500 (1988).

[23] J. Wang, J. Onuchic, and P. Wolynes, Phys. Rev. Lett. **76**, 4861 (1996); H. E. Castillo and P. Le Doussal, *ibid.* **86**, 4859 (2001).

[24] S. Tretiak, V. Chernyak, and S. Mukamel, J. Phys. Chem. B **102**, 3310 (1998).

[25] S. Tretiak, V. Chernyak, and S. Mukamel, Phys. Rev. Lett. **77**, 4656 (1996).

[26] M. E. J. Newman, e-print, cond-mat/0001118, and references therein.

[27] L. Valkunas, G. Trinkunas, and V. Liuolia, in *Resonance Energy Transfer*, edited by D. L. Andrews and A. A. Demidov (Wiley, New York, 1999).